

# Accurate autocorrelation modeling substantially improves fMRI reliability

Wiktor Olszowy<sup>a</sup>, John Aston<sup>b</sup>, Catarina Rua<sup>a</sup>, Guy B. Williams<sup>a</sup>

<sup>a</sup>Wolfson Brain Imaging Centre, Department of Clinical Neurosciences, University of Cambridge, Cambridge, United Kingdom

<sup>b</sup>Statistical Laboratory, Department of Pure Mathematics and Mathematical Statistics, University of Cambridge, Cambridge, United Kingdom

---

## Abstract

Given the recent controversies in some neuroimaging statistical methods, we compared the most frequently used functional Magnetic Resonance Imaging (fMRI) analysis packages: AFNI, FSL and SPM, with regard to temporal autocorrelation modeling. This process, sometimes known as pre-whitening, is conducted in virtually all task fMRI studies. We employed eleven datasets containing 980 scans corresponding to different fMRI protocols and subject populations. Though autocorrelation modeling in AFNI was not perfect, its performance was much higher than the performance of autocorrelation modeling in FSL and SPM. The residual autocorrelated noise in FSL and SPM led to heavily confounded first level results, particularly for low-frequency experimental designs. Also, we observed very severe problems for scans with short repetition times. The resulting false positives and false negatives can be expected to propagate to the group level, especially if the group analysis is performed with a mixed effects model. Our results show superior performance of SPM's alternative pre-whitening: FAST, over the default SPM's method. The reliability of task fMRI studies would increase with more accurate autocorrelation modeling. Furthermore, reliability could increase if the analysis packages provided diagnostic plots. This way the investigator would be aware of residual autocorrelated noise in the GLM residuals. We provide a MATLAB script for the fMRI researchers to check if their analyses might be affected by imperfect pre-whitening.

*Keywords:* fMRI, statistics, methods validation, temporal autocorrelation

---

## 1 Introduction

2 Functional Magnetic Resonance Imaging (fMRI) data is  
3 known to be positively autocorrelated in time (Bullmore et al.,  
4 1996). It results from neural sources, but also from scanner-  
5 induced low-frequency drifts, respiration and cardiac pulsation,  
6 as well as from movement artefacts not accounted for by motion  
7 correction (Lund et al., 2006). If this autocorrelation is not ac-  
8 counted for, spuriously high fMRI signal at one time point can  
9 be prolonged to the subsequent time points, which increases  
10 the likelihood of obtaining false positives in task studies. As a  
11 result, parts of the brain might erroneously appear active dur-  
12 ing an experiment. The degree of temporal autocorrelation is  
13 different across the brain (Worsley et al., 2002). In particular,  
14 autocorrelation in gray matter is stronger than in white matter  
15 and cerebrospinal fluid, but it also varies within gray matter.

16 AFNI (Cox, 1996), FSL (Jenkinson et al., 2012) and  
17 SPM (Penny et al., 2011), the most popular packages used  
18 in fMRI research, first remove the signal at very low fre-  
19 quencies (for example using a high-pass filter), after which  
20 they estimate the residual temporal autocorrelation and re-  
21 move it in a process called pre-whitening. In AFNI tempo-  
22 ral autocorrelation is modeled voxel-wise. For each voxel,  
23 an autoregressive-moving-average ARMA(1,1) model is esti-  
24 mated. The ARMA(1,1) estimates are not spatially smoothed.  
25 For FSL, a Tukey taper is used to smooth the spectral density

estimates voxel-wise. These smoothed estimates are then ad-  
26 ditionally smoothed within tissue type. Woolrich et al. (2001)  
27 showed the appropriateness of the FSL's method for two fMRI  
28 protocols: with repetition time (TR) of 1.5s and of 3s, and with  
29 voxel size  $4 \times 4 \times 7 \text{ mm}^3$ . By default, SPM estimates temporal  
30 autocorrelation globally as an autoregressive AR(1) plus white  
31 noise process (Purdon and Weisskoff, 1998). SPM has an alter-  
32 native approach: FAST, but we know of only two studies which  
33 have used it (Todd et al., 2016; Bollmann et al., 2018). Boll-  
34 mann et al. (2018) explains FAST uses a dictionary of covari-  
35 ance components based on exponential covariance functions. 36

37 In Lenoski et al. (2008) several fMRI autocorrelation model-  
38 ing approaches were compared for one fMRI protocol (TR=3s,  
39 voxel size  $3.75 \times 3.75 \times 4 \text{ mm}^3$ ). The authors found that the  
40 use of the global AR(1), of the spatially smoothed AR(1) and  
41 of the spatially smoothed FSL-like noise models resulted in  
42 worse whitening performance than the use of the non-spatially  
43 smoothed noise models. Eklund et al. (2012) showed that in  
44 SPM the shorter the TR, the more likely it is to get false posi-  
45 tive results in first level (also known as single subject) analyses.  
46 It was argued that SPM often does not remove a substantial part  
47 of the autocorrelated noise. The relationship between shorter  
48 TR and increased false positive rates was also shown in Purdon  
49 and Weisskoff (1998) for the case when autocorrelation was not  
50 accounted for.

51 In this study we investigated the whitening performance of  
52 AFNI, FSL and SPM for a wide variety of fMRI protocols.  
53 We analyzed both the default SPM's method and the alternative

---

Email address: wo222@cam.ac.uk (Wiktor Olszowy)

Table 1: Overview of the employed datasets. FCP = Functional Connectomes Project. NKI = Nathan Kline Institute. BMMR = Biomedical Magnetic Resonance. CRIC = Cambridge Research into Impaired Consciousness. CamCAN = Cambridge Centre for Ageing and Neuroscience. For the Enhanced NKI data, only scans from release 3 were used. Out of the 46 subjects in release 3, scans of 30 subjects were taken. For the rest, at least one scan was missing. For the BMMR data, there were 7 subjects at 3 sessions, resulting in 21 scans. For the CamCAN data, 200 subjects were considered only.

Study	Experiment	Place	Design	No. subjects	Field [T]	TR [s]	Voxel size [mm]	No. voxels	Time points
FCP	resting state	Beijing	N/A	198	3	2	3.1x3.1x3.6	64x64x33	225
	resting state	Cambridge, US	N/A	198	3	3	3x3x3	72x72x47	119
NKI	resting state	Orangeburg, US	N/A	30	3	1.4	2x2x2	112x112x64	404
	resting state	Orangeburg, US	N/A	30	3	0.645	3x3x3	74x74x40	900
CRIC	resting state	Cambridge, UK	N/A	73	3	2	3x3x3.8	64x64x32	300
neuRosim	resting state	(simulated)	N/A	100	NA	2	3.1x3.1x3.6	64x64x33	225
NKI	checkerboard	Orangeburg, US	20s off+20s on	30	3	1.4	2x2x2	112x112x64	98
	checkerboard	Orangeburg, US	20s off+20s on	30	3	0.645	3x3x3	74x74x40	240
BMMR	checkerboard	Magdeburg	12s off+12s on	21	7	3	1x1x1	182x140x45	80
CRIC	checkerboard	Cambridge, UK	16s off+16s on	70	3	2	3x3x3.8	64x64x32	160
CamCAN	sensorimotor	Cambridge, UK	event-related	200	3	1.97	3x3x4.44	64x64x32	261

54 one: FAST. Furthermore, we analyzed the resulting specificity-  
55 sensitivity trade-offs in first level fMRI results. The main part of  
56 the paper compares the pre-whitening approaches from AFNI,  
57 FSL and SPM for boxcar experimental designs. Supplementary  
58 material includes analysis of an event-related design dataset, as  
59 well as a group level comparison of SPM's default method with  
60 FAST. We observed better whitening performance for AFNI and  
61 SPM tested with option FAST than for FSL and SPM. Imperfect  
62 pre-whitening heavily confounded first level analyses.

## 63 Data

64 In order to explore a range of parameters that may affect  
65 autocorrelation, we investigated 11 fMRI datasets (Table 1).  
66 These included resting state and task studies, healthy subjects  
67 and a patient population, different TRs, magnetic field strengths  
68 and voxel sizes. We also used anatomical MRI scans, as they  
69 were needed for the registration of brains to the MNI (Montreal  
70 Neurological Institute) atlas space. FCP (Biswal et al., 2010),  
71 NKI (Nooner et al., 2012) and CamCAN data (Shafto et al.,  
72 2014) are publicly shared anonymized data. Data collection at  
73 the respective sites was subject to their local institutional review  
74 boards (IRBs), who approved the experiments and the dissemination  
75 of the anonymized data. For the 1,000 Functional Connectomes  
76 Project (FCP), collection of the Beijing data was approved by  
77 the IRB of State Key Laboratory for Cognitive Neuroscience and  
78 Learning, Beijing Normal University; collection of the Cambridge  
79 data was approved by the Massachusetts General Hospital partners  
80 IRB. For the Enhanced NKI Rockland Sample, collection and dissemination  
81 of the data was approved by the NYU School of Medicine IRB. For  
82 the analysis of an event-related design dataset, which can be found  
83 in Supplementary material, we used the CamCAN dataset (Cambridge  
84 Centre for Ageing and Neuroscience, [www.cam-can.org](http://www.cam-can.org)). Ethical  
85 approval for the study was obtained from the Cambridgeshire 2  
86 (now East of England - Cambridge Central) Research Ethics

Committee. The study from Magdeburg ("BMMR checker-  
88 board") (Hamid et al., 2015) was approved by the IRB of the  
89 Otto von Guericke University, and the scans have not been  
90 made public yet. The study of Cambridge Research into Im-  
91 paired Consciousness (CRIC) was approved by the Cambridge  
92 Local Research Ethics Committee (99/391), and the scans have  
93 not been made public yet. In all studies all subjects or their  
94 consultees gave informed written consent after the experimental  
95 procedures were explained. One rest dataset consisted of simu-  
96 lated data generated with the neuRosim package in R (Welvaert  
97 et al., 2011). Simulation details can be found in Supplementary  
98 material.  
99

## 100 Methods

101 For AFNI, FSL and SPM analyses, the preprocessing, brain  
102 masks, brain registrations to the 2 mm isotropic MNI atlas  
103 space, and multiple comparison corrections were kept consis-  
104 tent (Fig. 1). This way we limited the influence of possible  
105 confounders on the results. In order to investigate whether our  
106 results are an artefact of the comparison approach used for as-  
107 sessment, we compared AFNI, FSL and SPM by investigating  
108 (1) the power spectra of the GLM residuals, (2) the spatial dis-  
109 tribution of significant clusters, (3) the average percentage of  
110 significant voxels within the brain mask, and (4) the positive  
111 rate: proportion of subjects with at least one significant cluster.  
112 The power spectrum represents the variance of a signal that is  
113 attributable to an oscillation of a given frequency. When calcu-  
114 lating the power spectra of the GLM residuals, we considered  
115 voxels in native space using the same brain mask for AFNI, FSL  
116 and SPM. For each voxel, we normalized the time series to have  
117 variance 1 and calculated the power spectra as the square of the  
118 discrete Fourier transform.

119 Apart from assuming dummy designs for resting state data  
120 as in Eklund et al. (2012, 2015, 2016), we also assumed wrong  
121 (dummy) designs for task data, and we used resting state scans

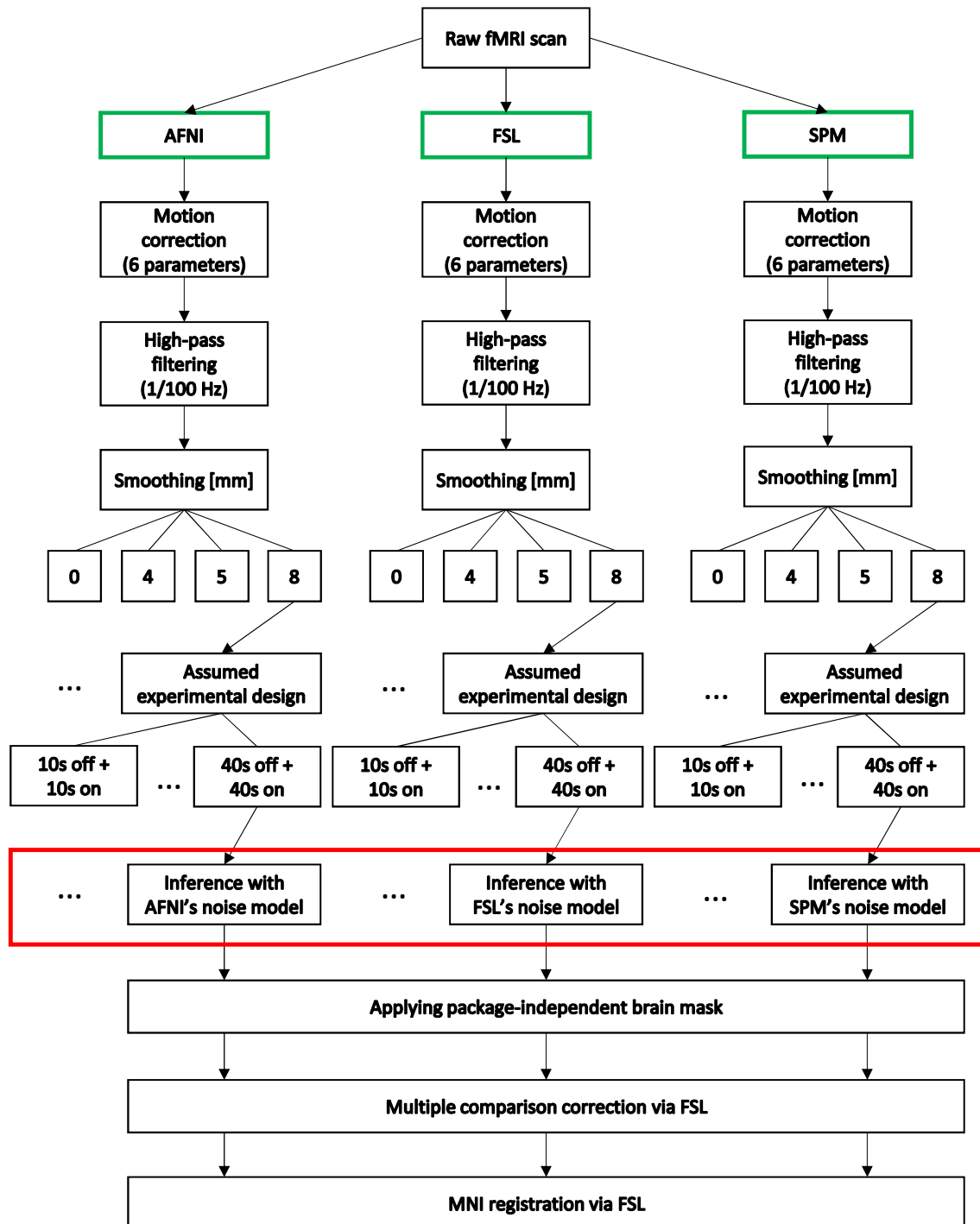


Figure 1: The employed analyses pipelines. The noise models used by AFNI, FSL and SPM were the only relevant difference (marked in a red box).

122 simulated using the neuRosim package in R (Welvaert et al.,  
 123 2011). We treated such data as null data. For null data, the  
 124 positive rate is the familywise error rate, which was employed  
 125 in Eklund et al. (2012, 2015, 2016). We use the term “signif-  
 126 icant voxel” to denote a voxel that is covered by one of the  
 127 clusters returned by the multiple comparison correction.

128 All the processing scripts needed to fully replicate our  
 129 study are at [https://github.com/wiktorolszowy/fMRI\\_](https://github.com/wiktorolszowy/fMRI_)

temporal\_autocorrelation. We used AFNI 16.2.02, FSL  
 5.0.10 and SPM 12 (v7219).

### Preprocessing

132 Slice timing correction was not performed, as for some  
 133 datasets the slice timing information was not available. In each  
 134 of the three packages we performed motion correction, which  
 135 resulted in 6 parameters that we considered as confounders in  
 136

137 the consecutive statistical analysis. Furthermore, in each of the  
138 three packages we conducted high-pass filtering with frequency  
139 cut-off of 1/100 Hz. We performed registration to MNI space  
140 only within FSL. For AFNI and SPM, the results of the multi-  
141 ple comparison correction were registered to MNI space using  
142 transformations generated by FSL. First, anatomical scans were  
143 brain extracted with FSL's brain extraction tool (BET) (Smith,  
144 2002). Then, FSL's boundary based registration (BBR) was  
145 used for registration of the fMRI volumes to the anatomical  
146 scans. The anatomical scans were aligned to 2 mm isotropic  
147 MNI space using affine registration with 12 degrees of freedom.  
148 The two transformations were then combined for each subject  
149 and saved for later use in all analyses, including in those started  
150 in AFNI and SPM. Gaussian spatial smoothing was performed  
151 in each of the packages separately.

### 152 *Statistical analysis*

153 For analyses in each package, we used the canonical hemo-  
154 dynamic response function (HRF) model, also known as the  
155 double gamma model. It is implemented the same way in  
156 AFNI, FSL and SPM: the response peak is set at 5 seconds  
157 after stimulus onset, while the post-stimulus undershoot is set  
158 at around 15 seconds after onset. This function was combined  
159 with each of the assumed designs using the convolution func-  
160 tion. To account for possible response delays and different slice  
161 acquisition times, we used in the three packages the first deriva-  
162 tive of the double gamma model, also known as the temporal  
163 derivative. We did not incorporate physiological recordings to  
164 the analysis pipeline, as these were not available for most of the  
165 datasets used.

166 We estimated the statistical maps in each package sepa-  
167 rately. AFNI, FSL and SPM use Restricted Maximum Like-  
168 lihood (ReML), where autocorrelation is estimated given the  
169 residuals from an initial Ordinary Least Squares (OLS) model  
170 estimation. The ReML procedure then pre-whitens both the  
171 data and the design matrix, and estimates the model. We con-  
172 tinued the analysis with the statistic maps corresponding to the  
173 t-test with null hypothesis being that the full regression model  
174 without the canonical HRF explains as much variance as the  
175 full regression model with the canonical HRF. All three pack-  
176 ages produced brain masks. The statistic maps in FSL and SPM  
177 were produced within the brain mask only, while in AFNI the  
178 statistic maps were produced for the entire volume. We masked  
179 the statistic maps from AFNI, FSL and SPM using the inter-  
180 sected brain masks from FSL and SPM. We did not confine the  
181 analyses to a gray matter mask, because autocorrelation is at  
182 strongest in gray matter (Worsley et al., 2002). In other words,  
183 false positives caused by imperfect pre-whitening can be ex-  
184 pected to occur mainly in gray matter. By default, AFNI and  
185 SPM produced t-statistic maps, while FSL produced both t- and  
186 z-statistic maps. In order to transform the t-statistic maps to z-  
187 statistic maps, we extracted the degrees of freedom from each  
188 analysis output.

189 Next, we performed multiple comparison correction in FSL  
190 for all the analyses, including for those started in AFNI and  
191 SPM. First, we estimated the smoothness of the brain-masked  
192 4-dimensional residual maps using the `smoothest` function

193 in FSL. Knowing the DLH parameter, which describes image  
194 roughness, and the number of voxels within the brain mask  
195 (VOLUME), we then ran the `cluster` function in FSL on the  
196 z-statistic maps using a cluster defining threshold of 3.09 and  
197 significance level of 5%. This is the default multiple compar-  
198 ison correction in FSL. Finally, we applied previously saved  
199 MNI transformations to the binary maps which were showing  
200 the location of the significant clusters.

## 201 **Results**

### 202 *Whitening performance of AFNI, FSL and SPM*

203 To investigate the whitening performance resulting from  
204 the use of noise models in AFNI, FSL and SPM, we plotted  
205 the power spectra of the GLM residuals. Fig. 2 shows the  
206 power spectra averaged across all brain voxels and subjects for  
207 smoothing of 8 mm and assumed boxcar design of 10s of rest  
208 followed by 10s of stimulus presentation. The statistical infer-  
209 ence in AFNI, FSL and SPM relies on the assumption that the  
210 residuals after pre-whitening are white. For white residuals, the  
211 power spectra should be flat. However, for all the datasets and  
212 all the packages, there was some visible structure. The strongest  
213 artefacts were visible for FSL and SPM at low frequencies. At  
214 high frequencies, power spectra from FAST were closer to 1  
215 than power spectra from the other methods. Fig. 2 does not  
216 show respiratory spikes which one could expect to see. This  
217 is because the figure refers to averages across subjects. We ob-  
218 served respiratory spikes when analyzing power spectra for sin-  
219 gle subjects (not shown). Importantly, for the “BMMR checker-  
220 board” dataset analyzed both with the default SPM's method  
221 and with FAST, there was a small peak at frequency 1/24 Hz,  
222 which was the true design frequency. For AFNI and FSL, this  
223 peak was higher. As the assumed design was a wrong design,  
224 a low power spectrum at the true design frequency suggests too  
225 strong pre-whitening, during which negative autocorrelations  
226 can be introduced.

### 227 *Resulting specificity-sensitivity trade-offs*

228 In order to investigate the impact of the whitening perfor-  
229 mance on first level results, we analyzed the spatial distribution  
230 of significant clusters in AFNI, FSL and SPM. Fig. 3 shows  
231 an exemplary axial slice in the MNI space for 8 mm smooth-  
232 ing. It was made through the imposition of subjects' bina-  
233 rized significance masks on each other. Scale refers to the per-  
234 centage of subjects within a dataset where significant activa-  
235 tion was detected at the given voxel. The x-axis corresponds  
236 to four assumed designs. Resting state data was used as null  
237 data. Thus, low numbers of significant voxels were a desir-  
238 able outcome, as this was suggesting high specificity. Task  
239 data with assumed wrong designs was used as null data too.  
240 Thus, clear differences between the true design (indicated with  
241 red boxes) and the wrong designs were a desirable outcome.  
242 For FSL and SPM, often the relationship between lower as-  
243 sumed design frequency (“boxcar40” vs. “boxcar12”) and an  
244 increased number of significant voxels was visible, in particu-  
245 lar for the resting state datasets: “FCP Beijing”, “FCP Cam-  
246 bridge” and “CRIC”. For null data, significant clusters in AFNI

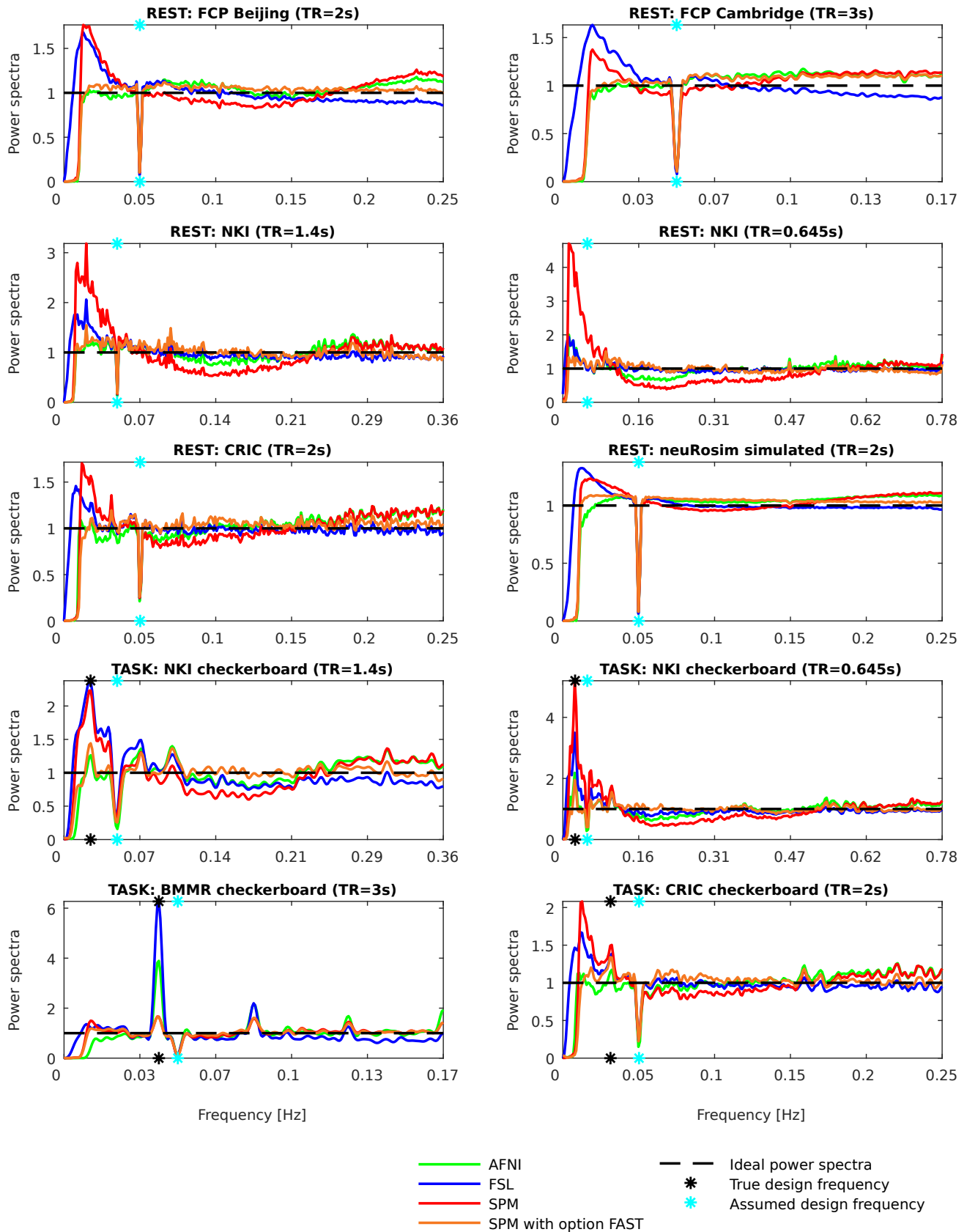


Figure 2: Power spectra of the GLM residuals in native space averaged across brain voxels and across subjects for the assumed boxcar design of 10s of rest followed by 10s of stimulus presentation (“boxcar10”). The dips at 0.05 Hz are due to the assumed design period being 20s (10s + 10s). For some datasets, the dip is not seen as the assumed design frequency was not covered by one of the sampled frequencies. The frequencies on the x-axis go up to the Nyquist frequency, which is 0.5/TR. If after pre-whitening the residuals were white (as it is assumed), the power spectra would be flat. AFNI and SPM’s alternative method: FAST, led to best whitening performance (most flat spectra). For FSL and SPM, there was substantial autocorrelated noise left after pre-whitening, particularly at low frequencies.

247 were scattered primarily within gray matter. For FSL and SPM, 302  
248 many significant clusters were found in the posterior cingulate 303  
249 cortex, while most of the remaining significant clusters were 304  
250 scattered within gray matter across the brain. False positives in 305  
251 gray matter occur due to the stronger positive autocorrelation 306  
252 in this tissue type compared to white matter (Worsley et al., 307  
253 2002). For the task datasets: “NKI checkerboard TR=1.4s”, 308  
254 “NKI checkerboard TR=0.645s”, “BMMR checkerboard” and 309  
255 “CRIC checkerboard” tested with the true designs, the majority 310  
256 of significant clusters were located in the visual cortex. This re- 311  
257 sulted from the use of visual experimental designs for the fMRI 312  
258 task. For the impaired consciousness patients (“CRIC”), the 313  
259 registrations to MNI space were imperfect, as the brains were 314  
260 often deformed. 315

### 261 *Additional comparison approaches*

262 The above analysis referred to the spatial distribution of sig- 316  
263 nificant clusters on an exemplary axial slice. As the results can 317  
264 be confounded by the comparison approach, we additionally in- 318  
265 vestigated two other comparison approaches: the percentage of 319  
266 significant voxels and the positive rate. Supplementary materi- 320  
267 al, Fig. S1 shows the average percentage of significant voxels 321  
268 across subjects in 10 datasets for smoothing of 8 mm and for 16 322  
269 assumed boxcar experimental designs. As more designs were 323  
270 considered, the relationship between lower assumed design fre- 324  
271 quency and an increased percentage of significant voxels in FSL 325  
272 and SPM (discussed before for Fig. 3) was even more appar- 326  
273 ent. This relationship was particularly interesting for the “CRIC 327  
274 checkerboard” dataset. When tested with the true design, the 328  
275 percentage of significant voxels for AFNI, FSL, SPM and FAST 329  
276 was similar: 1.2%, 1.2%, 1.5% and 1.3%, respectively. How- 330  
277 ever, AFNI and FAST returned much lower percentages of sig- 331  
278 nificant voxels for the assumed wrong designs. For the assumed 332  
279 wrong design “40”, FSL and SPM returned a higher percentage 333  
280 of significant voxels than for the true design: 1.4% and 2.2%, 334  
281 respectively. Results for AFNI and FAST for the same design 335  
282 showed only 0.3% and 0.4% of significantly active voxels. For 336  
283 the “BMMR checkerboard” dataset tested with the true design, 337  
284 SPM and FAST resulted in a much lower percentage of signif- 338  
285 icant voxels than AFNI and FSL. The average percentage of 339  
286 significant voxels across subjects for this dataset tested with the 340  
287 true design was 31.5% for AFNI, 36.7% for FSL, 6.7% for SPM 341  
288 and 7.6% for FAST, respectively. This agrees with Fig. 3. For 342  
289 this dataset, the brain mask was limited mainly to the occipi- 343  
290 tal lobe and the percentage relates to the field of view that was 344  
291 used. For this dataset, the power spectrum at the true design 345  
292 was much lower for SPM and FAST than for AFNI and FSL 346  
293 (Fig. 2). This suggests negative autocorrelations were intro- 347  
294 duced during pre-whitening for the assumed true design. This 348  
295 led to a decrease in perceived activation. 349

296 Overall, at an 8 mm smoothing level, AFNI and FAST out- 350  
297 performed FSL and SPM showing a lower average percentage 351  
298 of significant voxels in tests with the wrong design: on average 352  
299 across 10 datasets and across the wrong designs, the average 353  
300 percentage of significant voxels was 0.4% for AFNI, 1% for 354  
301 FSL, 1.9% for SPM and 0.3% for FAST. 355

As multiple comparison correction depends on the smooth-  
ness level of the residual maps, we also checked the correspond-  
ing differences between AFNI, FSL and SPM. The residual  
maps seemed to be similarly smooth. At an 8 mm smoothing  
level, the average geometric mean of the estimated FWHMs of  
the Gaussian distribution in x-, y-, and z-dimensions across the  
10 datasets and across the 16 assumed designs was 10.8 mm for  
AFNI, 10.3 mm for FSL, 11.7 mm for SPM and 11.5 mm for  
FAST. Nonetheless, we also investigated the percentage of vox-  
els with z-statistic above 3.09. This value is the 99.9% quantile  
of the standard normal distribution and is often used as the clus-  
ter defining threshold. For null data, this percentage should be  
0.1%. The average percentage across the 10 datasets and across  
the wrong designs was 0.5% for AFNI, 1.2% for FSL, 2.1% for  
SPM and 0.4% for FAST.

Supplementary material, Figs. S2-S3 show the positive rate  
for smoothing of 4 and 8 mm. The general patterns resemble  
those already discussed for the percentage of significant vox-  
els, with AFNI and FAST consistently returning lowest posi-  
tive rates (familywise error rates) for resting state scans and  
task scans tested with wrong designs. For task scans tested  
with the true designs, the positive rates for the different pre-  
whitening methods were similar. The black horizontal lines  
show the 5% false positive rate, which is the expected pro-  
portion of scans with at least one significant cluster if in real-  
ity there was no experimentally-induced signal in the subject’s  
brain. The dashed horizontal lines are the confidence inter-  
vals for the proportion of false positives. These were calcu-  
lated knowing that variance of a Bernoulli( $p$ ) distributed ran-  
dom variable is  $p(1 - p)$ . Thus, the confidence intervals were  
 $0.05 \pm \sqrt{0.05 \cdot 0.95/n}$ , with  $n$  denoting the number of subjects  
in the dataset.

Since smoothing implicitly affects the voxel size, we con-  
sidered different smoothing kernel sizes. We chose 4, 5 and  
8 mm, as these are the defaults in AFNI, FSL and SPM. No  
smoothing was also considered, as for 7T data this preprocess-  
ing step is sometimes avoided (Walter et al., 2008; Polimeni  
et al., 2017). With a wider smoothing kernel, the percentage  
of significant voxels increased (not shown), while the posi-  
tive rate decreased. Differences between AFNI, FSL, SPM and  
FAST discussed above for the four comparison approaches and  
smoothing of 8 mm were consistent across the four smoothing  
levels.

## 345 **Discussion**

346 In the case of FSL and SPM for the datasets “FCP Bei- 347  
348 jing”, “FCP Cambridge”, “CRIC RS” and “CRIC checker- 348  
349 board”, there was a clear relationship between lower assumed 349  
350 design frequency and an increased percentage of significant 350  
351 voxels. Purdon and Weisskoff (1998) showed that this relation- 351  
352 ship exists when positive autocorrelation is not removed from 352  
353 the data. This phenomenon is caused by the spurious signal 353  
354 spillage. If during the assumed activation period the noise pro- 354  
355 cess spuriously takes high values and the assumed design fre- 355  
quency is high, due to the residual positive autocorrelation we

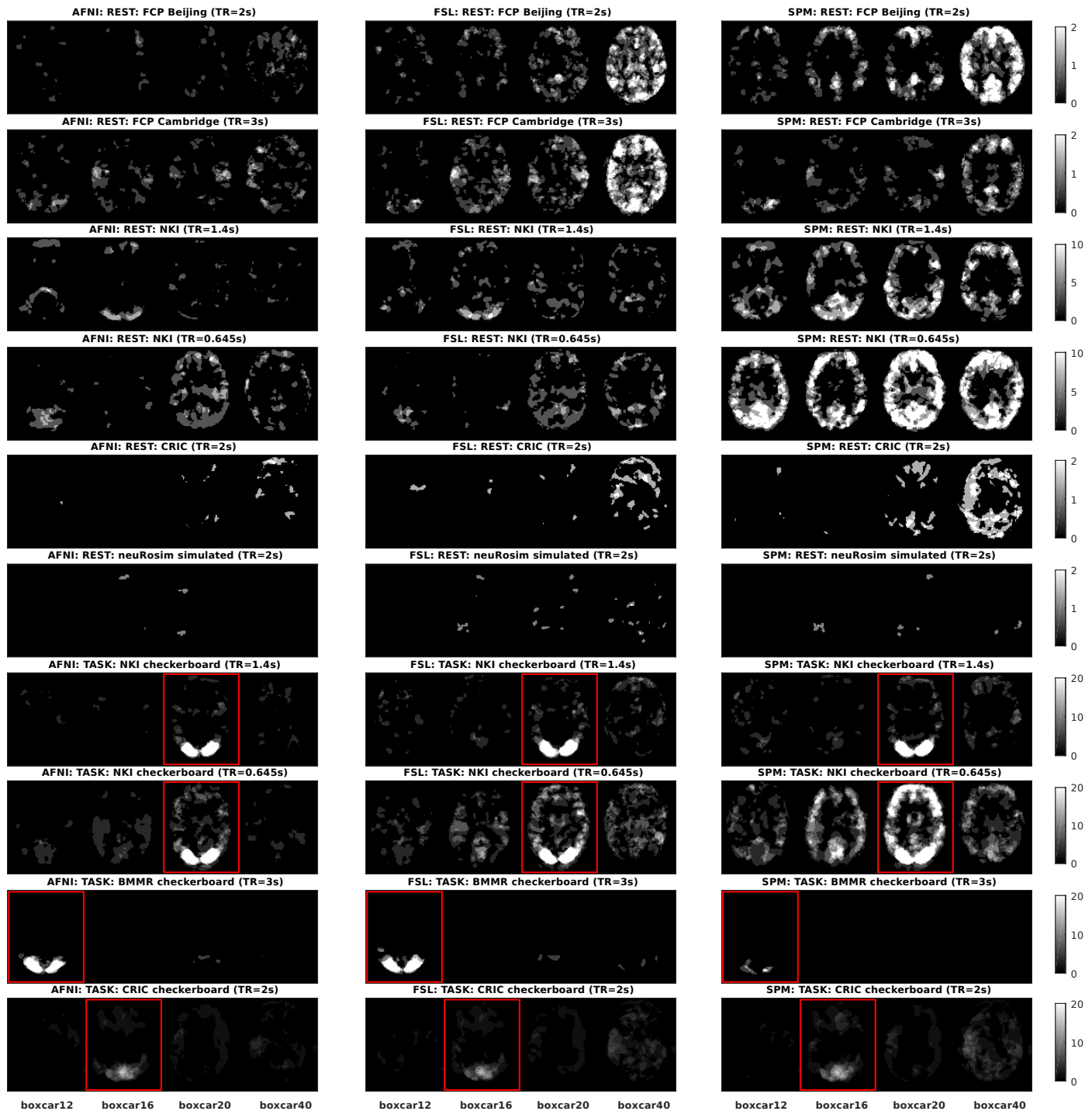


Figure 3: Spatial distribution of significant clusters in AFNI (left), FSL (middle) and SPM (right) for different assumed experimental designs. Scale refers to the percentage of subjects where significant activation was detected at the given voxel. The red boxes indicate the true designs (for task data). Resting state data was used as null data. Thus, low numbers of significant voxels were a desirable outcome, as it was suggesting high specificity. Task data with assumed wrong designs was used as null data too. Thus, large positive differences between the true design and the wrong designs were a desirable outcome. The clearest cut between the true and the wrong/dummy designs was obtained with AFNI's noise model. FAST performed similarly to AFNI's noise model (not shown).

356 can expect higher signal values during the beginning of the assumed  
 357 assumed rest period. Thus, it will be difficult to distinguish the  
 358 assumed activation period from the assumed rest period, and  
 359 the spuriously high signal during the former period will likely  
 360 not result in detected significance. On the other hand, if such a

361 spuriously high signal occurs in the middle of a long assumed  
 362 activation period, there will be enough time for the signal to re-  
 363 turn to its baseline level, so that there will be a larger difference  
 364 between the mean signal during the assumed activation period  
 365 and the mean signal during the assumed rest period. As a result,

366 detection of significant activation will be more likely.

367 An interesting case was the checkerboard experiment con- 423  
368 ducted with impaired consciousness patients, where FSL and 424  
369 SPM found a higher percentage of significant voxels for the de- 425  
370 sign with the assumed lowest design frequency than for the true 426  
371 design. As this subject population was unusual, one might sus- 427  
372 pect weaker or inconsistent response to the stimulus. However, 428  
373 positive rates for this experiment for the true design were all 429  
374 around 50%, substantially above other assumed designs. 430

375 Compared to FSL and SPM, the use of AFNI's and FAST 431  
376 noise models for task datasets resulted in larger differences be- 432  
377 tween the true design and the wrong designs in the first level 433  
378 results. This occurred because of more accurate autocorrelation 434  
379 modeling in AFNI and in FAST. In our analyses FSL and SPM 435  
380 left a substantial part of the autocorrelated noise in the data and 436  
381 the statistics were biased. For none of the pre-whitening ap- 437  
382 proaches were the positive rates around 5%, which was the sig- 438  
383 nificance level used in the cluster inference. This is likely due to 439  
384 imperfect cluster inference in FSL. High familywise error rates 440  
385 in first level FSL analyses were already reported in Eklund et al. 441  
386 (2015). In our study the familywise error rate following the use 442  
387 of AFNI's and FAST noise models was consistently lower than 443  
388 the familywise error rate following the use of FSL's and SPM's 444  
389 noise models. Opposed to the average percentage of significant 445  
390 voxels, high familywise error rate directly points to problems 446  
391 in the modeling of many subjects. 447

392 The highly significant responses for the NKI datasets are in 448  
393 line with Eklund et al. (2012), where it was shown that for fMRI 449  
394 scans with short TR it is more likely to detect significant activa- 450  
395 tion. The NKI scans that we considered had TR of 0.645s and 451  
396 1.4s, in both cases much shorter than the usual repetition times. 452  
397 Such short repetition times are now possible due to multiband 453  
398 sequences (Larkman et al., 2001). The shorter the TR, the 454  
399 higher the correlations between adjacent time points (Purdon 455  
400 and Weisskoff, 1998). If positive autocorrelation in the data 456  
401 is higher than the estimated level, then false positive rates will 457  
402 increase. The study of Eklund et al. (2012) only referred to 458  
403 SPM. In addition to the previous study, we observed that the 459  
404 familywise error rate for short TRs was substantially lower in 460  
405 FSL than in SPM, though still much higher than for resting 461  
406 state scans at TR=2s ("FCP Beijing" and "CRIC RS"). FSL 462  
407 models autocorrelation more flexibly than SPM, which seems 463  
408 to be confirmed by our study. For short TRs, AFNI's perfor- 464  
409 mance deteriorated too, as autocorrelation spans more than one 465  
410 TR (Bollmann et al., 2018) and an ARMA(1,1) noise model can 466  
411 only partially capture it. 467

412 Apart from the different TRs, we analyzed the impact of spa- 468  
413 tial smoothing. If more smoothing is applied, the signal from 469  
414 gray matter will be often mixed with the signal from white mat- 470  
415 ter. As autocorrelation in white matter is lower than in gray mat- 471  
416 ter (Worsley et al., 2002), autocorrelation in a primarily gray 472  
417 matter voxel will likely decrease following stronger smoothing. 473  
418 The observed relationships of the percentage of significant vox- 474  
419 els and of the positive rate from the smoothing level can be sur- 475  
420 prising, as random field theory is believed to account for differ- 476  
421 ent levels of data smoothness. The relationship for the positive 477  
422 rate (familywise error rate) was already shown in Eklund et al.

(2012, 2015). More about the impact of smoothing and spatial 423  
resolution can be found in Geissler et al. (2005); Weibull et al. 424  
(2008); Mueller et al. (2017). We considered smoothing only 425  
as a confounder. Importantly, for all four levels of smoothing, 426  
AFNI and FAST outperformed FSL and SPM. 427

428 Compared to FSL, the use of SPM resulted in a lower per- 429  
centage of significant voxels for the "FCP Cambridge" and 430  
"BMMR checkerboard" datasets. These were the only datasets 431  
with TR of more than 2 seconds. For the "FCP Cambridge" 432  
dataset, a lower percentage of significant voxels was a desirable 433  
result, as the dataset was used as null data. However, compared 434  
to AFNI and FSL, SPM was less sensitive in detecting activa- 435  
tion in the primary visual cortex for the "BMMR checkerboard" 436  
dataset. Because the autocorrelation modeling approach in 437  
SPM has little flexibility, in case of long TR, where the correla- 438  
tions between adjacent time points become smaller, SPM might 439  
introduce negative autocorrelations during pre-whitening. For 440  
boxcar designs, this lowers the statistics and increases false neg- 441  
ative rates (Lenoski et al., 2008). Surprisingly, compared to 442  
AFNI and FSL, for the "BMMR checkerboard" dataset tested 443  
with the true design, the use of FAST also led to a lower per- 444  
centage of significant voxels. 445

446 Our results confirm Lenoski et al. (2008) insofar as our study 447  
also showed best performance of a method that did not involve 448  
spatial smoothing of the autocorrelation parameters. Interest- 449  
ingly, in Eklund et al. (2015) AFNI, FSL and SPM were already 450  
compared in the context of first level fMRI analyses. AFNI re- 451  
sulted in substantially lower false positive rates than FSL and 452  
slightly lower false positive rates than SPM. We also observed 453  
lowest false positive rates for AFNI. Opposed to Eklund et al. 454  
(2015), which compared the packages in their entirety, we com- 455  
pared the packages only with regard to pre-whitening. It is 456  
possible that pre-whitening is the most crucial single difference 457  
between AFNI, FSL and SPM, and that the relationships de- 458  
scribed in Eklund et al. (2015) would look completely different 459  
if AFNI, FSL and SPM employed the same pre-whitening. For 460  
one dataset, Eklund et al. (2015) also observed that SPM led to 461  
worst whitening performance. 462

463 We did not perform slice timing correction, but to account 464  
for different slice acquisition times we employed the temporal 465  
derivative. The differences in first level results between AFNI, 466  
FSL and SPM which we observed could have been smaller 467  
if physiological recordings had been modeled. The modeling 468  
of physiological noise is known to improve whitening perfor- 469  
mance, particularly for short TRs (Lund et al., 2006; Bollmann 470  
et al., 2018). Unfortunately, cardiac and respiratory signals are 471  
not always acquired in fMRI studies. Even less often are the 472  
physiological recordings incorporated to the analysis pipeline. 473

474 *How to explain pre-whitening problems in FSL and SPM?* 475

476 FSL provided a benchmarking paper of its pre-whitening ap- 477  
proach (Woolrich et al., 2001). The study employed data cor- 478  
responding to two fMRI protocols. For one protocol TR was 479  
1.5s, while for the other protocol TR was 3s. For both proto- 480  
cols, the voxel size was 4x4x7 mm<sup>3</sup>. These were large voxels. 481  
We suspect that the FSL's pre-whitening approach could have 482  
been overfitted to this data. 483



479 Friston et al. (2000) and Lenoski et al. (2008) showed that  
480 pre-whitening with a global noise model can result in profound  
481 bias. SPM's default is a global noise model. However, SPM's  
482 problems could be partially related to the estimation procedure.  
483 Firstly, the estimation is approximative as it uses a Taylor ex-  
484 pansion (Friston et al., 2002). Secondly, the estimation is based  
485 on a subset of the voxels. Only voxels with  $p < 0.001$  follow-  
486 ing inference with no pre-whitening are selected. This means  
487 that the estimation strongly depends both on the TR and on the  
488 experimental design (Purdon and Weisskoff, 1998).

#### 489 *Impact on group studies*

490 If the second level analysis is performed with a random  
491 effects model, the standard error maps are not used. Thus,  
492 random effects models like the summary statistic approach in  
493 SPM should not be affected by imperfect pre-whitening (Fris-  
494 ton et al., 2005). On the other hand, residual positive autocor-  
495 related noise decreases the signal differences between the acti-  
496 vation blocks and the rest blocks. This is particularly relevant  
497 for event-related designs (see Supplementary material). Bias  
498 from confounded coefficient maps can be expected to propa-  
499 gate to the group level. In Supplementary material we showed  
500 that pre-whitening indeed confounds group analyses performed  
501 with a random effects model. However, more relevant is the  
502 case of mixed effects analyses, for example when using 3dMEMA  
503 in AFNI (Chen et al., 2012) or FLAME in FSL (Woolrich et al.,  
504 2004). These approaches additionally employ standard error  
505 maps, which are also confounded by imperfect pre-whitening.  
506 Bias in mixed effects fMRI analyses resulting from non-white  
507 noise at the first level was already reported in Bianciardi et al.  
508 (2004). We postulate that more accurate autocorrelation mod-  
509 eling at the subject level can substantially improve fMRI reli-  
510 ability both at the subject level and at the group level.

#### 511 *What is the best null data for fMRI methods validation studies?*

512 For resting state data treated as task data, it is possible to  
513 observe activation both in the posterior cingulate cortex and  
514 in the frontal cortex, since these regions belong to the default  
515 mode network (Raichle et al., 2001). In fact, in Supplemen-  
516 tary Figure 18 in Eklund et al. (2016) the spatial distribution  
517 plots of significant clusters indicate that the significant clusters  
518 appear mainly in the posterior cingulate cortex, even though  
519 the assumed design for that analysis was a randomized event-  
520 related design. The rest activity in these regions can occur at  
521 different frequencies and can underlie different patterns (Stark  
522 and Squire, 2001). Thus, resting state data is not perfect null  
523 data for task fMRI analyses, especially if one uses an approach  
524 where a subject with one small cluster in the posterior cingu-  
525 late cortex enters an analysis with the same weight as a subject  
526 with a number of large clusters spread throughout the entire  
527 brain. Task fMRI data is not perfect null data either, as an as-  
528 sumed wrong design might be confounded by the underlying  
529 true design. For simulated data, a consensus is needed how  
530 to model autocorrelation, spatial dependencies, physiological  
531 noise, scanner-dependent low-frequency drifts and head mo-  
532 tion. Some of the current simulation toolboxes (Welvaert and

Rossee, 2014) enable the modeling of all these aspects of fMRI  
533 data, but as the later analyses might heavily depend on the spe-  
534 cific choice of parameters, more work is needed to understand  
535 how the different sources of noise influence each other. In our  
536 study, results for simulated resting state data were substantially  
537 different compared to acquired real resting state scans. In par-  
538 ticular, the percentage of significant voxels for the simulated  
539 data was much lower, indicating that the simulated data did  
540 not appropriately correspond to the underlying brain physiolo-  
541 gy. Considering resting state data where the posterior cingu-  
542 late cortex and the frontal cortex are masked out could be an  
543 alternative null. Because there is no perfect fMRI null data,  
544 we used both resting state data with assumed dummy designs  
545 and task data with assumed wrong designs. Results for both  
546 approaches coincided.  
547

#### 548 *Conclusions*

549 Using data corresponding to a wide variety of fMRI proto-  
550 cols, we showed that AFNI and SPM tested with option FAST  
551 had the best whitening performance, followed by FSL and  
552 SPM. Pre-whitening in FSL and SPM left substantial resid-  
553 ual autocorrelated noise in the data, primarily at low frequen-  
554 cies. Though the problems were most severe for short repetition  
555 times, all considered fMRI protocols were affected. We showed  
556 that the residual autocorrelated noise led to heavily confounded  
557 first level results. Low-frequency boxcar designs were affected  
558 the most. Due to better whitening performance, it was much  
559 easier to distinguish the assumed true experimental design from  
560 the assumed wrong experimental designs with AFNI and FAST  
561 than with FSL and SPM. This suggests superior specificity-  
562 sensitivity trade-off resulting from the use of AFNI's and FAST  
563 noise models. The differences between AFNI, FSL and SPM  
564 were large and consistent across four different comparison ap-  
565 proaches and across 11 datasets. The resulting false positives  
566 and false negatives can be expected to propagate to the group  
567 level, especially if the group analysis is performed with a mixed  
568 effects model. Results derived from FSL could be made more  
569 robust if a different autocorrelation model was applied. How-  
570 ever, currently there is no alternative pre-whitening approach in  
571 FSL. For SPM, our findings support more widespread use of the  
572 FAST method. Unfortunately, although the vast majority of task  
573 fMRI analyses is conducted with linear regression, the popular  
574 analysis packages do not provide diagnostic plots. For old ver-  
575 sions of SPM, the external toolbox SPMd generated them (Luo  
576 and Nichols, 2003). It provided a lot of information, which  
577 paradoxically could have limited its popularity. We believe that  
578 task fMRI analyses would strongly benefit if AFNI, FSL and  
579 SPM provided some basic diagnostic plots. This way the inves-  
580 tigator would be aware, for example, of residual autocorrelated  
581 noise in the GLM residuals. We provide a MATLAB script  
582 (GitHub: `plot_power_spectra_of_GLM_residuals.m`) for  
583 the fMRI researchers to check if their analyses might be af-  
584 fected by imperfect pre-whitening.  
585

## Acknowledgments

We would like to thank Paul Browne, Anders Eklund, Thomas Nichols, Karl Friston, Richard Reynolds, Paola Fiano, Adrian Carpenter, Alison Sleight, Gang Chen, Guillaume Flandin, and Michał Kosicki for much valuable advice. Furthermore, we would like to thank the James S. McDonnell Foundation for funding the image acquisitions of the Cambridge Research into Impaired Consciousness (CRIC) group, and the CRIC group for sharing their data. Oliver Speck, Michael Hoffmann and Aini Ismafairus from the Otto von Guericke University provided us with the 7T data. We also thank the Neuroimaging Informatics Tools and Resources Clearinghouse and all of the researchers who have contributed with data to the 1,000 Functional Connectomes Project and to the Enhanced Nathan Kline Institute - Rockland Sample. W.O. was in receipt of scholarships from the Cambridge Trust and from the Mateusz B. Grabowski Fund.

## References

Bianciardi, M., Cerasa, A., Patria, F., Hagberg, G., 2004. Evaluation of mixed effects in event-related fMRI studies: impact of first-level design and filtering. *NeuroImage* 22 (3), 1351–1370.

Biswal, B. B., Mennes, M., Zuo, X.-N., Gohel, S., Kelly, C., Smith, S. M., Beckmann, C. F., Adelstein, J. S., Buckner, R. L., Colcombe, S., et al., 2010. Toward discovery science of human brain function. *Proceedings of the National Academy of Sciences* 107 (10), 4734–4739.

Bollmann, S., Puckett, A. M., Cunnington, R., Barth, M., 2018. Serial correlations in single-subject fMRI with sub-second TR. *NeuroImage* 166, 152 – 166.

Bullmore, E., Brammer, M., Williams, S. C., Rabe-Hesketh, S., Janot, N., David, A., Mellers, J., Howard, R., Sham, P., 1996. Statistical methods of estimation and inference for functional MR image analysis. *Magnetic Resonance in Medicine* 35 (2), 261–277.

Buračas, G. T., Boynton, G. M., 2002. Efficient design of event-related fMRI experiments using M-sequences. *NeuroImage* 16 (3), 801–813.

Chen, G., Saad, Z. S., Nath, A. R., Beauchamp, M. S., Cox, R. W., 2012. FMRI group analysis combining effect estimates and their variances. *NeuroImage* 60 (1), 747–765.

Cox, R. W., 1996. AFNI: software for analysis and visualization of functional magnetic resonance neuroimages. *Computers and Biomedical research* 29 (3), 162–173.

Eklund, A., Andersson, M., Josephson, C., Johansson, M., Knutsson, H., 2012. Does parametric fMRI analysis with SPM yield valid results? – An empirical study of 1484 rest datasets. *NeuroImage* 61 (3), 565–578.

Eklund, A., Nichols, T., Andersson, M., Knutsson, H., 2015. Empirically investigating the statistical validity of SPM, FSL and AFNI for single subject fMRI analysis. In: *Biomedical Imaging (ISBI), 2015 IEEE 12th International Symposium on*. IEEE, pp. 1376–1380.

Eklund, A., Nichols, T. E., Knutsson, H., 2016. Cluster failure: Why fMRI inferences for spatial extent have inflated false-positive rates. *Proceedings of the National Academy of Sciences*, 201602413.

Friston, K., Josephs, O., Zarahn, E., Holmes, A., Rouquette, S., Poline, J.-B., 2000. To smooth or not to smooth?: Bias and efficiency in fMRI time-series analysis. *NeuroImage* 12 (2), 196–208.

Friston, K. J., Glaser, D. E., Henson, R. N., Kiebel, S., Phillips, C., Ashburner, J., 2002. Classical and Bayesian inference in neuroimaging: applications. *NeuroImage* 16 (2), 484–512.

Friston, K. J., Stephan, K. E., Lund, T. E., Morcom, A., Kiebel, S., 2005. Mixed-effects and fMRI studies. *NeuroImage* 24 (1), 244–252.

Geissler, A., Lanzenberger, R., Barth, M., Tahamant, A. R., Milakara, D., Gartus, A., Beisteiner, R., 2005. Influence of fMRI smoothing procedures on replicability of fine scale motor localization. *NeuroImage* 24 (2), 323–331.

Hamid, A. I. A., Speck, O., Hoffmann, M. B., 2015. Quantitative assessment of visual cortex function with fMRI at 7 Tesla—test-retest variability. *Frontiers in Human Neuroscience* 9.

Jenkinson, M., Beckmann, C. F., Behrens, T. E., Woolrich, M. W., Smith, S. M., 2012. FSL. *NeuroImage* 62 (2), 782–790.

Larkman, D. J., Hajnal, J. V., Herlihy, A. H., Coutts, G. A., Young, I. R., Ehnholm, G., 2001. Use of multicoil arrays for separation of signal from multiple slices simultaneously excited. *Journal of Magnetic Resonance Imaging* 13 (2), 313–317.

Lenoski, B., Baxter, L. C., Karam, L. J., Maisog, J., Debbs, J., 2008. On the performance of autocorrelation estimation algorithms for fMRI analysis. *IEEE Journal of Selected Topics in Signal Processing* 2 (6), 828–838.

Lund, T. E., Madsen, K. H., Sidaros, K., Luo, W.-L., Nichols, T. E., 2006. Non-white noise in fMRI: does modelling have an impact? *NeuroImage* 29 (1), 54–66.

Luo, W.-L., Nichols, T. E., 2003. Diagnosis and exploration of massively univariate neuroimaging models. *NeuroImage* 19 (3), 1014–1032.

Mueller, K., Lepsien, J., Möller, H. E., Lohmann, G., 2017. Commentary: Cluster failure: Why fMRI inferences for spatial extent have inflated false-positive rates. *Frontiers in Human Neuroscience* 11, 345.

Nooner, K. B., Colcombe, S. J., Tobe, R. H., Mennes, M., Benedict, M. M., Moreno, A. L., Panek, L. J., Brown, S., Zavitz, S. T., Li, Q., et al., 2012. The NKI-Rockland sample: a model for accelerating the pace of discovery science in psychiatry. *Frontiers in Neuroscience* 6.

Penny, W. D., Friston, K. J., Ashburner, J. T., Kiebel, S. J., Nichols, T. E., 2011. *Statistical parametric mapping: the analysis of functional brain images*. Academic press.

Polimeni, J. R., Renvall, V., Zaretskaya, N., Fischl, B., 2017. Analysis strategies for high-resolution UHF-fMRI data. *NeuroImage*.

Purdon, P. L., Weiskoff, R. M., 1998. Effect of temporal autocorrelation due to physiological noise and stimulus paradigm on voxel-level false-positive rates in fMRI. *Human Brain Mapping* 6 (4), 239–249.

Raichle, M. E., MacLeod, A. M., Snyder, A. Z., Powers, W. J., Gusnard, D. A., Shulman, G. L., 2001. A default mode of brain function. *Proceedings of the National Academy of Sciences* 98 (2), 676–682.

Shafto, M. A., Tyler, L. K., Dixon, M., Taylor, J. R., Rowe, J. B., Cusack, R., Calder, A. J., Marslen-Wilson, W. D., Duncan, J., Dalgleish, T., et al., 2014. The Cambridge Centre for Ageing and Neuroscience (Cam-CAN) study protocol: a cross-sectional, lifespan, multidisciplinary examination of healthy cognitive ageing. *BMC Neurology* 14 (1), 204.

Smith, S. M., 2002. Fast robust automated brain extraction. *Human Brain Mapping* 17 (3), 143–155.

Stark, C. E., Squire, L. R., 2001. When zero is not zero: the problem of ambiguous baseline conditions in fMRI. *Proceedings of the National Academy of Sciences* 98 (22), 12760–12766.

Todd, N., Moeller, S., Auerbach, E. J., Yacoub, E., Flandin, G., Weiskopf, N., 2016. Evaluation of 2D multiband EPI imaging for high-resolution, whole-brain, task-based fMRI studies at 3T: Sensitivity and slice leakage artifacts. *NeuroImage* 124, 32–42.

Walter, M., Stadler, J., Tempelmann, C., Speck, O., Northoff, G., 2008. High resolution fMRI of subcortical regions during visual erotic stimulation at 7 T. *Magnetic Resonance Materials in Physics, Biology and Medicine* 21 (1), 103–111.

Weibull, A., Gustavsson, H., Mattsson, S., Svensson, J., 2008. Investigation of spatial resolution, partial volume effects and smoothing in functional MRI using artificial 3D time series. *NeuroImage* 41 (2), 346–353.

Welvaert, M., Durnez, J., Moerkerke, B., Verdoolaege, G., Rosseel, Y., 2011. neuRosim: An R package for generating fMRI data. *Journal of Statistical Software* 44 (10), 1–18.

Welvaert, M., Rosseel, Y., 2014. A review of fMRI simulation studies. *PLOS ONE* 9 (7), e101953.

Woolrich, M. W., Behrens, T. E., Beckmann, C. F., Jenkinson, M., Smith, S. M., 2004. Multilevel linear modelling for FMRI group analysis using Bayesian inference. *NeuroImage* 21 (4), 1732–1747.

Woolrich, M. W., Ripley, B. D., Brady, M., Smith, S. M., 2001. Temporal autocorrelation in univariate linear modeling of FMRI data. *NeuroImage* 14 (6), 1370–1386.

Worsley, K. J., Liao, C., Aston, J., Petre, V., Duncan, G., Morales, F., Evans, A., 2002. A general statistical analysis for fMRI data. *NeuroImage* 15 (1), 1–15.

## 716 **Supplementary material**

### 717 *Simulation*

718 We used the `neuRosim` package to simulate 100 resting state  
719 scans. The `neuRosim` simulations account for white noise, tem-  
720 poral noise, low-frequency scanner-induced noise, physiologi-  
721 cal noise, task-related noise and spatial noise. Spatial noise  
722 captures spatial relationships in the data: that time series from  
723 voxels next to each other tend to be similar. The user specifies  
724 the weights of different noises. We arbitrarily chose a weight  
725 of 25% corresponding to white noise, a weight of 50% corre-  
726 sponding to temporal noise and a weight of 25% corresponding  
727 to spatial noise. For several other tested weights, we could not  
728 detect significant activation in any of the 100 simulated scans.  
729 `neuRosim` provides  $AR(m)$  models to account for temporal au-  
730 tocorrelation. The same model, i.e. with the same parameters,  
731 is used for each voxel. We decided to generate the temporally  
732 autocorrelated noise with the help of an  $AR(1)$  model. For the  
733 simulation procedure, a 3-dimensional baseline image must be  
734 provided by the user. The voxel-wise means in the simulated  
735 scans are equal to this baseline image. We chose a subject from  
736 the “FCP Beijing” dataset, subject ID “sub98617”, as the base-  
737 line subject. The baseline image used for the simulation was  
738 the average of the real scan over time. Scanning parameters are  
739 shown in Table 1. The number of time points was also chosen  
740 as in “FCP Beijing”. For the real “FCP Beijing” scan, we arbi-  
741 trarily chose a cuboidal region of interest, where we calculated  
742 the average parameter of voxel-wise  $AR(1)$  models. In the sim-  
743 ulation procedure it was not possible to directly use the  $AR(1)$   
744 parameter from the real “FCP Beijing” scan, as white noise and  
745 spatial noise influence the effective value of the parameter of  
746 the  $AR(1)$  model. That is why we found a parameter for the  
747 `neuRosim`’s  $AR(1)$  model so that the resulting average  $AR(1)$   
748 parameter in the simulated scans in the same cuboidal region of  
749 interest was very similar.

### 750 *Impact on event-related design studies*

751 In order to check if differences in autocorrelation model-  
752 ing in AFNI, FSL and SPM lead to different first level re-  
753 sults for event-related design studies, we analyzed the Cam-  
754 CAN dataset. The task was a sensorimotor one with visual and  
755 audio stimuli. The design included the stimulus m-sequence  
756 described in [Buračas and Boynton \(2002\)](#). Supplementary ma-  
757 terial, Fig. S4 shows (1) power spectra of the GLM residuals  
758 in native space averaged across brain voxels and across sub-  
759 jects for the assumed true design (“E1”), (2) average percentage  
760 of significant voxels for three wrong designs and the true de-  
761 sign, (3) positive rate for the same four designs, and (4) spatial  
762 distribution of significant clusters for the assumed true design  
763 (“E1”). Only smoothing of 8 mm was considered. The dummy  
764 event-related design (“E2”) consisted of relative stimulus onset  
765 times generated from a uniform distribution with limits 3s and  
766 6s. The stimulus duration times were 0.1s.

767 For the assumed low-frequency design (“B2”), AFNI’s auto-  
768 correlation modeling led to the lowest familywise error rate as  
769 residuals from FSL and SPM again showed a lot of signal at low  
770 frequencies. However, residuals from SPM tested with option

FAST were similar at low frequencies to AFNI’s residuals. As a  
result, the familywise error rate was similar to AFNI. For high  
frequencies, power spectra from SPM tested with option FAST  
were more closely around 1 than power spectra correspond-  
ing to the standard three approaches (AFNI/FSL/SPM). For an  
event-related design with very short stimulus duration times  
(around zero), residual positive autocorrelation at high frequen-  
cies makes it difficult to distinguish the activation blocks from  
the rest blocks, as part of the experimentally-induced signal is in  
the assumed rest blocks. This is what happened with AFNI and  
SPM. As their power spectra at high frequencies were above  
1, we observed a lower percentage of significant voxels com-  
pared to SPM tested with option FAST. On the other hand, FSL’s  
power spectra at high frequencies were below 1. As a result,  
FSL decorrelated activation blocks from rest blocks possibly  
introducing negative autocorrelations at high frequencies, lead-  
ing to a higher percentage of significant voxels than SPM tested  
with option FAST. Though we do not know the ground truth, we  
might expect that AFNI and SPM led for this event-related de-  
sign dataset to more false negatives than SPM with option FAST,  
while FSL led to more false positives. Alternatively, FSL might  
have increased the statistic values above their nominal levels for  
the truly but little active voxels.

### 794 *Impact on group studies with a random effects model*

795 To investigate the impact of pre-whitening on the group level,  
796 we performed in SPM random effects analyses for a one-sample  
797 t-test. We considered only the 8 mm smoothing level and results  
798 corresponding to SPM and FAST. As there were 10 datasets and  
799 16 assumed designs, for each pre-whitening we ran 160 group  
800 analyses. Four of these group analyses were for task data with  
801 assumed true design. The rest were analyses on null data. For  
802 null data, we found significant clusters in 14 analyses for SPM  
803 and in 16 analyses for FAST. This corresponded to a family-  
804 wise error rate of 9% for SPM and 10.3% for FAST. For task  
805 datasets tested with the true design, the use of FAST resulted in  
806 a lower percentage of significant voxels than the use of the de-  
807 fault method. For the NKI dataset at  $TR=1.4s$ , 6.5% of the  
808 brain was significant for SPM and 6.2% was significant for  
809 FAST. For the NKI dataset at  $TR=0.645s$ , SPM and FAST led  
810 to 7.1% and 6.4%, respectively. For the BMMR dataset, 10.8%  
811 and 10.7% of the brain was significant following the use of the  
812 default noise model of SPM and the use of FAST. For the “CRIC  
813 checkerboard” dataset, no significant clusters were found at the  
814 group level, as several of the subjects had deformed brains and  
815 the resulting group brain mask in MNI space did not cover the  
816 primary visual cortex.

817 Furthermore, we performed group analyses for the event-  
818 related design dataset: “CamCAN sensorimotor”. For the as-  
819 sumed true design, the use of FAST led to a higher percentage  
820 of significant voxels: 45.6% compared to 42.9% for the SPM’s  
821 default method. We observed the same relationship at the single  
822 subject level (Supplementary material, Fig. S4). While a high  
823 percentage of significant voxels might be surprising, the exper-  
824 iment included both visual and audio stimuli, and the dataset  
825 consisted of 200 subjects. A large number of subjects makes it  
826 easier to find significant activation if the effect size is negligible.

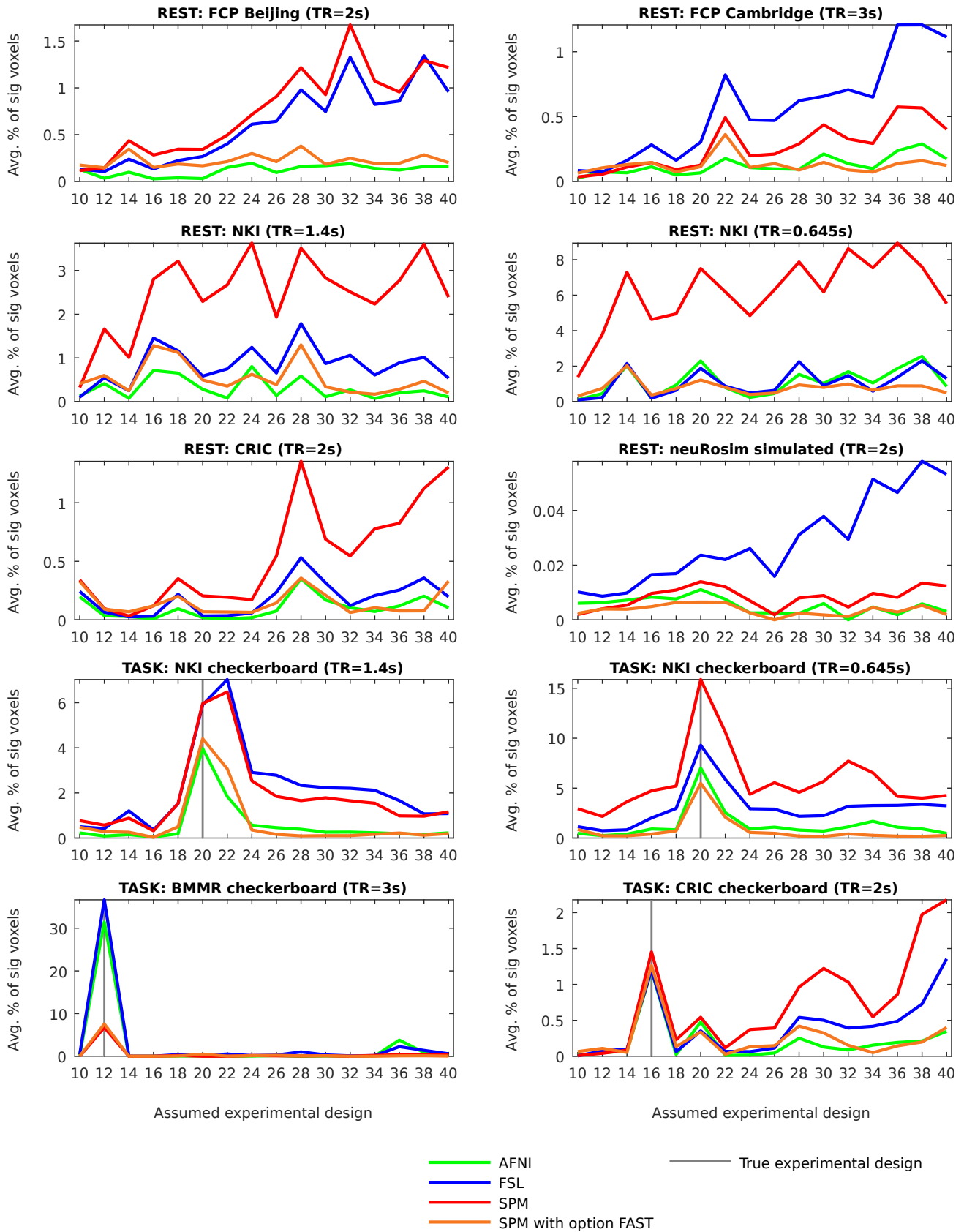


Figure S1: Average percentage of significant voxels across subjects for different packages. x-axis shows the assumed designs, e.g. “10” refers to the boxcar design of 10s of rest followed by 10s of stimulus presentation. Scans were spatially smoothed with FWHM of 8 mm. Resting state data was used as null data. Thus, a low percentage of significant voxels was a desirable outcome, as it was suggesting high specificity. Task data with assumed wrong designs was used as null data too. Thus, large positive differences between the true design and the wrong designs were a desirable outcome.

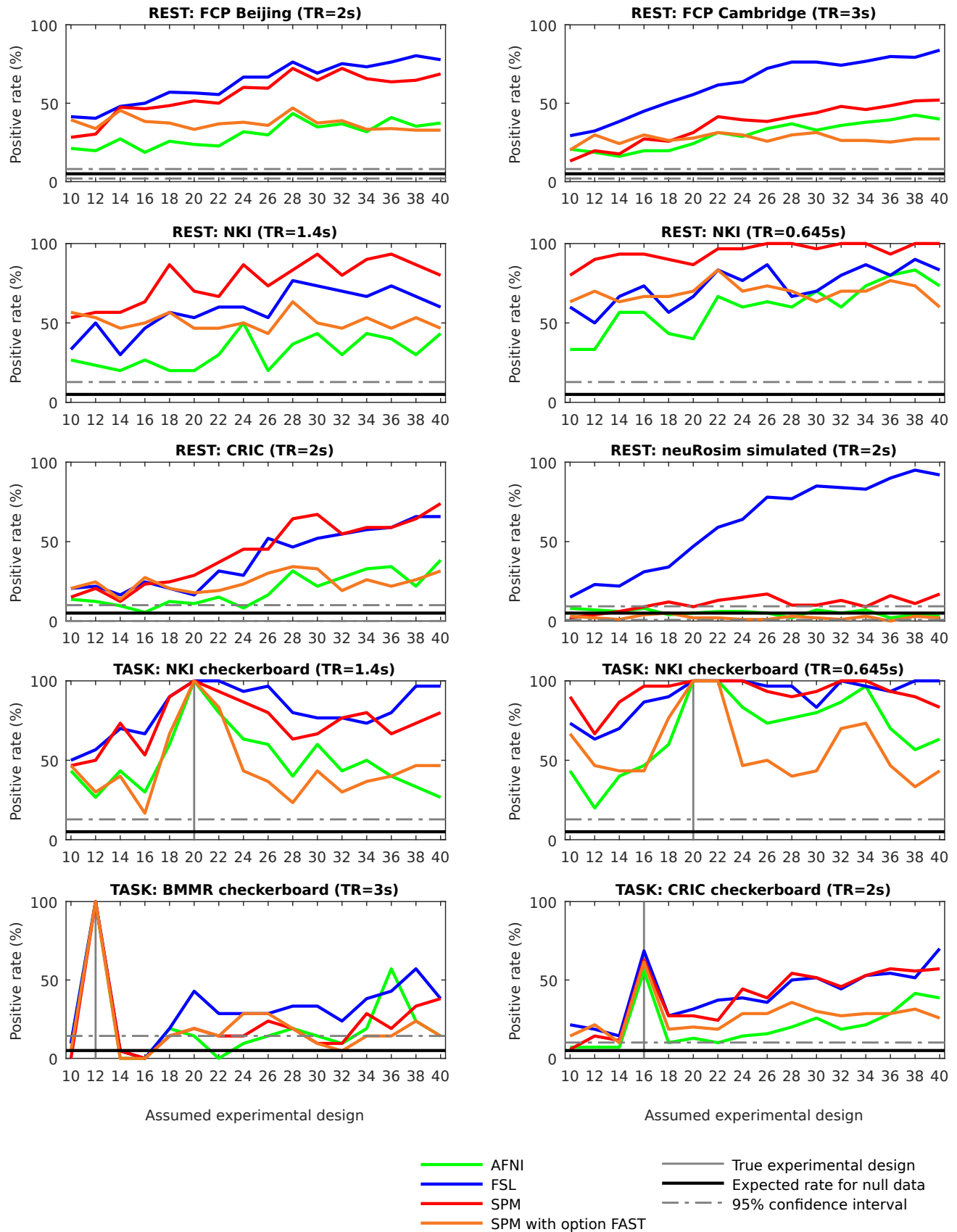


Figure S2: Positive rate for different packages. x-axis shows the assumed designs, e.g. “10” refers to the boxcar design of 10s of rest followed by 10s of stimulus presentation. Scans were spatially smoothed with FWHM of 4 mm. For null data, the positive rate is the familywise error rate. AFNI and FAST had the highest specificity.

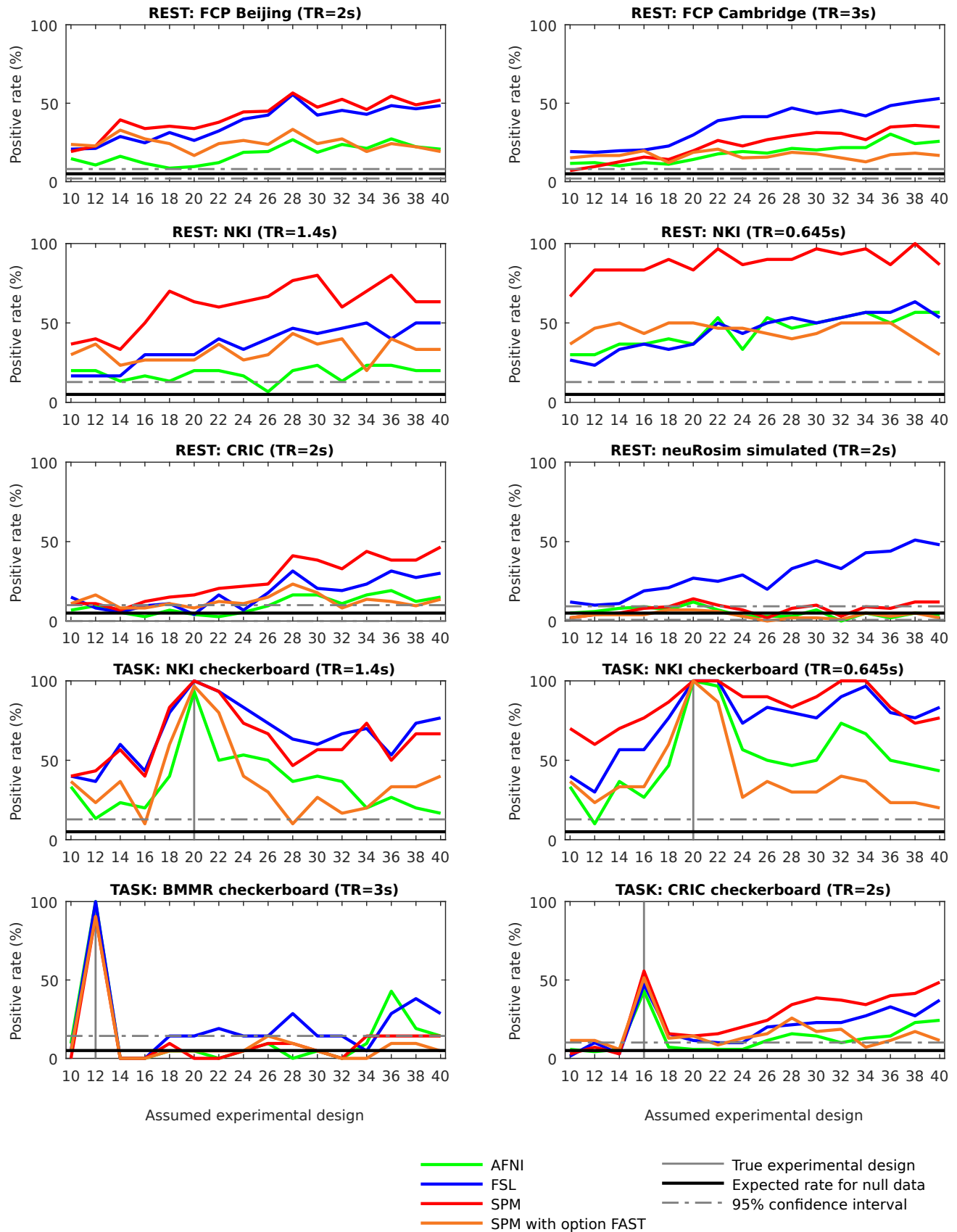


Figure S3: Positive rate for different packages. x-axis shows the assumed designs, e.g. “10” refers to the boxcar design of 10s of rest followed by 10s of stimulus presentation. Scans were spatially smoothed with FWHM of 8 mm. For null data, the positive rate is the familywise error rate. AFNI and FAST had the highest specificity.

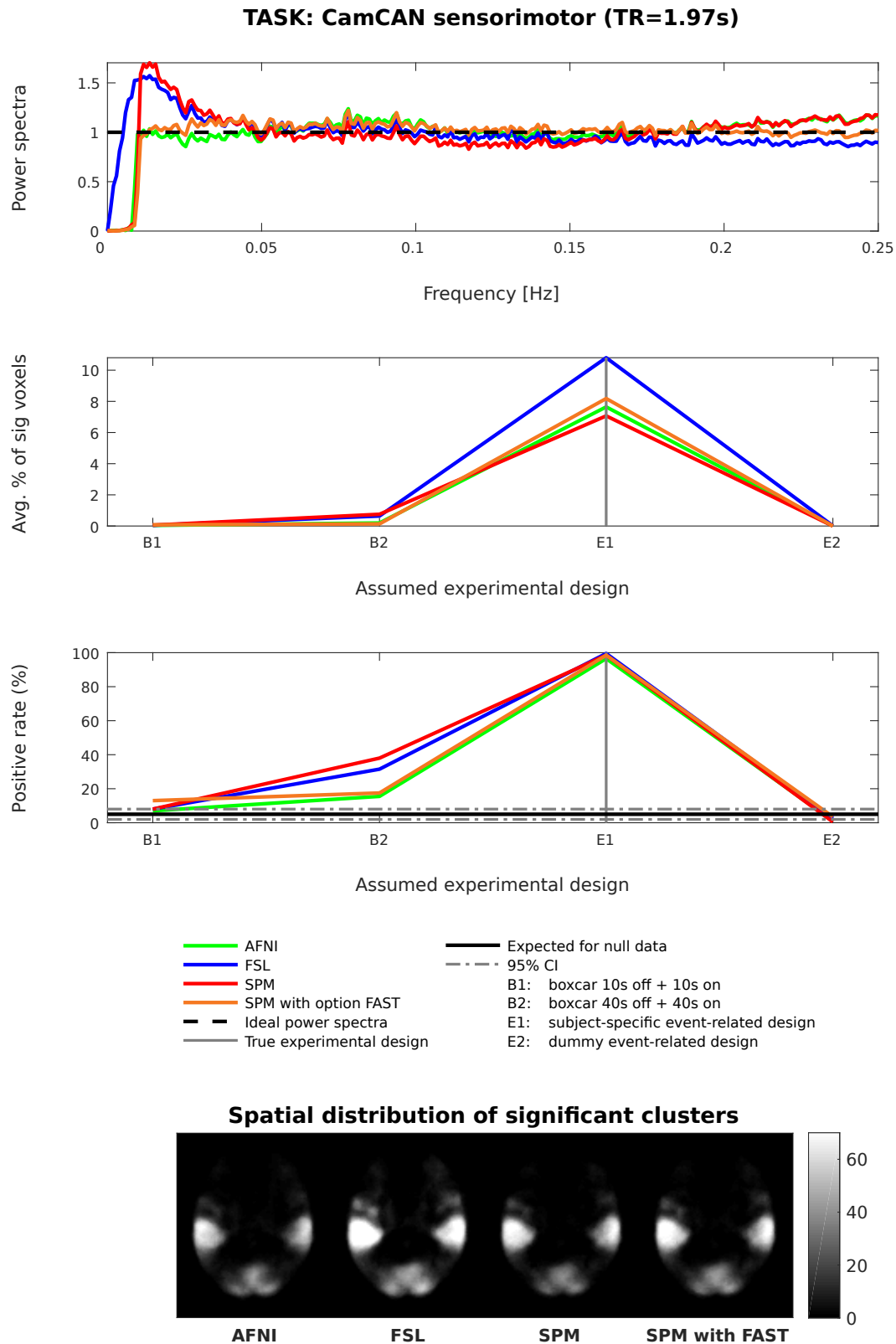


Figure S4: Differences between AFNI, FSL and SPM for a task dataset where the design was an event-related design (“CamCAN sensorimotor”). From top to bottom: (1) power spectra of the GLM residuals in native space averaged across brain voxels and across subjects for the assumed true design (“E1”), (2) average percentage of significant voxels for three wrong designs and the true design, (3) positive rate for the same four designs, and (4) spatial distribution of significant clusters for the assumed true design (“E1”) on an exemplary MNI axial slice. Scans were spatially smoothed with FWHM of 8 mm.